The Department of Scientific Computing

COMPUTATIONAL XPOSITION

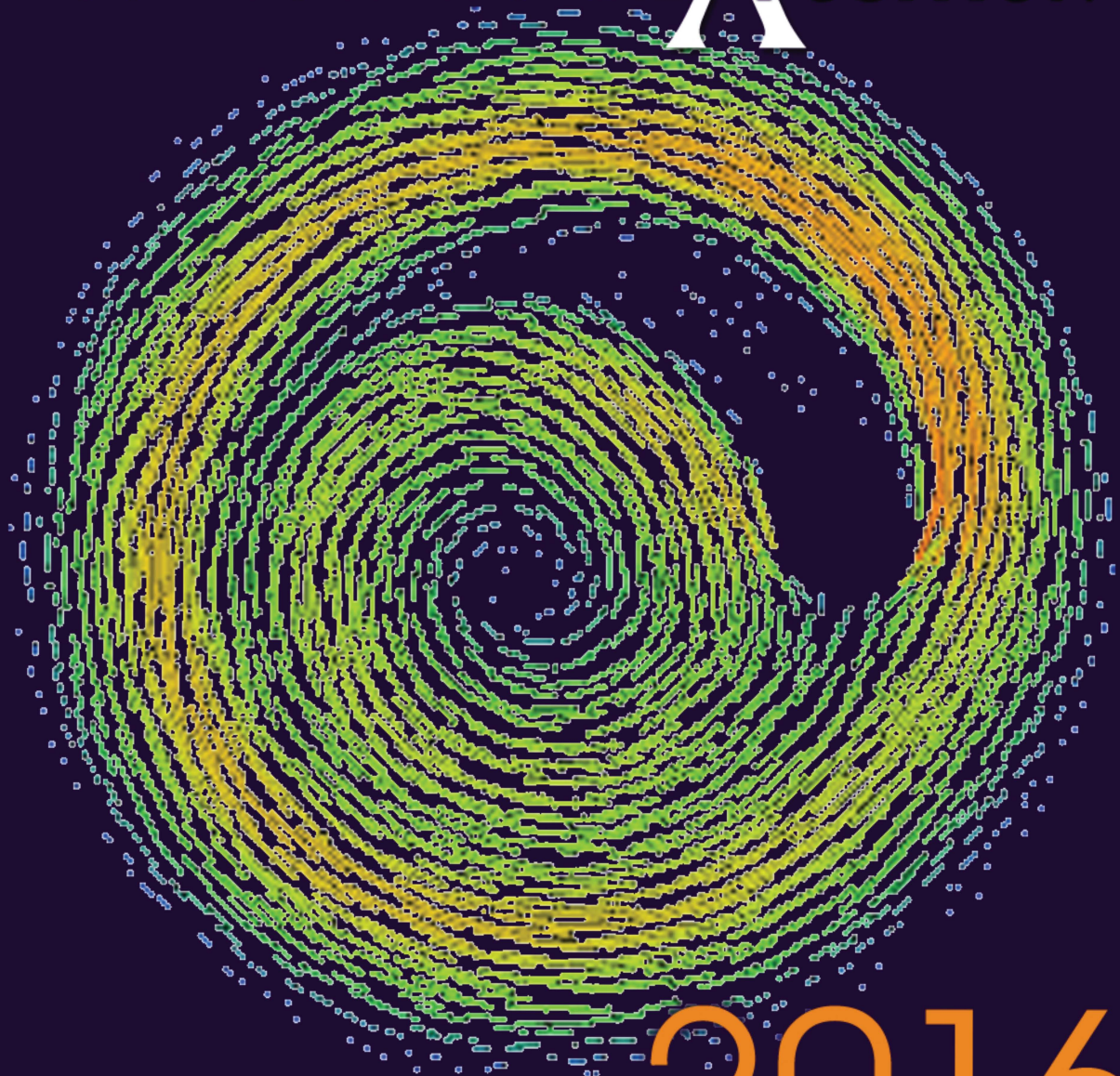

STUDENT PRESENTATIONS 2016

Welcome to Computational Xposition 2016, which showcases the research conducted by our students in the past year in the Department of Scientific Computing (DSC). Their research covers a broad spectrum of disciplines and blends computation, mathematics and applications. The innovation displayed in both algorithm development and their applications is quite broad and remarkable. Our students make us proud!

The student posters reflect the breadth and depth of the research carried out in the DSC. They are the direct result of a fulfilment of our two most important missions: providing world-class interdisciplinary research and training in computational science.

As we evolve our own graduate degree programs, the achievement of our students gives us confidence that we will succeed in becoming a premier institution for the training of the next generation of computational scientists. Indeed, looking at what our current students have achieved over the past several years serves as evidence that we are already there!

So, enjoy the presentations, interact with the students, quiz them, learn from them, and reflect on the fruits of their intelligence, skills, and labor, and join us in thanking them for their contributions to the DSC, to FSU, and to science.

Gordon Erlebacher
Chair, Department of Scientific Computing

Cover: Velocity field and mesh of the ensemble POD model, courtesy of Michael Schneier.

Presenting Students

STUDENT

Research

Philip Boehner
M.S. in Computational Science
Advisor: *Tomasz Plewa*

Nucleosynthesis using post-processing techniques

Our work focuses on improving a post-processing tool, Nucnet, to complement our grid-based Eulerian, finite volume hydrodynamics simulation code, Proteus. We simulate stellar evolution and supernova explosions with Proteus, but these inherently require the energy release from nucleosynthesis in order to drive the hydrodynamics evolution. The calculation of the nuclear reactions requires the computationally expensive solution to a highly nonlinear and stiff system of ODEs, the size of which is proportional to the number of isotopes present or that will be present in the simulated object. For this reason, we greatly reduce the number of participating isotopes to the few that most closely resemble the energy release provided by a larger, more complete set of isotopes. Unfortunately, this simplification also reduces the amount of isotopes available for comparison against observations. To recover the equivalent results with a higher number of participating isotopes, the hydrodynamics domain is seeded with a user-defined number of massless tracer particles that are advected using the grid velocity variables. These particles are responsible for recording the initial isotopic abundances of its underlying fluid element as well as its temperature and density evolution for the duration of the simulation. Following the completion of the simulation, we use our post-processing tool Nucnet to evolve each particle. Here the initial isotopic abundance distribution is evolved using the discrete temperature and density trajectory history with a larger number of participating isotopes. The spatial distribution of the particles coupled with the desired number of participating isotopes allows us to more closely compare our hydrodynamics results with observations. In this preliminary study we focus on the fundamental communication device between the two tools, the particle, and discuss the positional uncertainty introduced from advection, the optimal rate at which temperature and density information is recorded, and the minimum amount of particles required to sample an example domain. Future work will focus mainly on improving Nucnet in terms of flexibility, speed, and ease of use, in addition to further assessing the accuracy of our results.

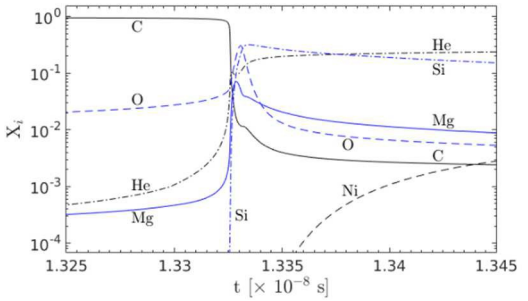

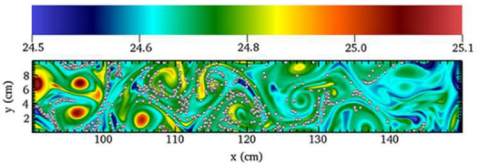

Figure 1, Left: Nuclear evolution of a fluid element over time
Figure 2, Above: Spatial variation of the average atomic mass, $\bar{A}$, for the final state of an example hydrodynamics simulation

Lukas Bystricky
Ph.D. in Computational Science
Advisors: *Janet Peterson & Sachin Shanbhag*

Computational fluid dynamics using the Deal.ii Finite Element Library

Computational fluid dynamics (CFD) encompasses a wide range of problems from aerodynamics to weather modelling. By far the most well known governing equations for CFD problems are the Navier-Stokes equations. This is a system of nonlinear partial differential equations. In general the Navier-Stokes equations can be very complicated to solve and depending on the problem, may involve a large number of degrees of freedom. Solving problems in CFD requires good numerical methods, one of which is the finite element method. The deal.ii C++ finite element library, currently maintained by Texas A&M University, provides many functions and routines to help efficiently set up, solve, and evaluate finite element problems. Using deal.ii and well established techniques in finite elements, we will compute solutions to the steady and unsteady incompressible Navier-Stokes equations and compare them to published benchmark problems. The problems considered will be the steady lid driven cavity problem, and computing lift and drag for unsteady flow past a cylinder.

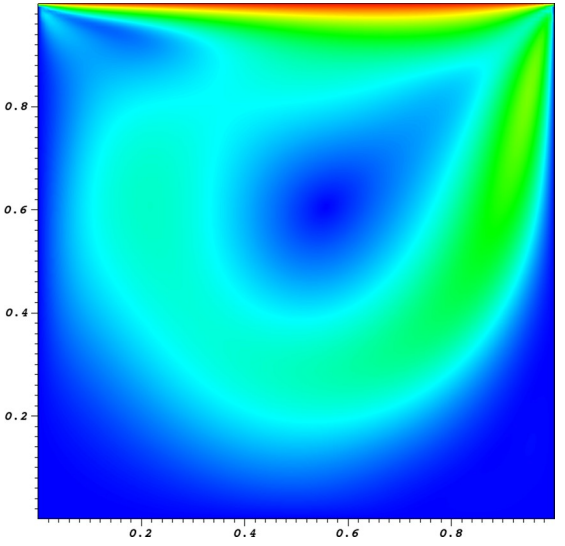

Figure 1, Above: Steady solution of the lid driven cavity problem at Reynolds number 400.

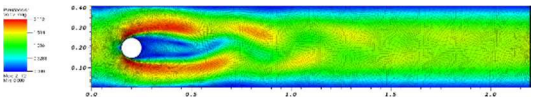

Figure 2, Right: Flow past a cylinder at Reynolds number 100.

Michael Conry
Ph.D. in Computational Science
Advisor: *Alan Lemmon*

Computational methods for determining genetic recombination's effect on phylogenetic analysis

Phylogenetic studies typically attempt to take into account as many evolutionary factors as possible to maintain accuracy. In practice, however, genetic recombination is often ignored entirely leading to questions regarding the accuracy of the resulting trees. Since genetic recombination can occur in any part of the genome, closely related individuals which should have the same underlying genetic history may appear more distantly related. Herein, we describe a novel computational method to help understand the impact of genetic recombination on phylogenetic analyses by simulating populations undergoing recombination and reproduction, then tracking the exons that are exchanged between chromosomes and individuals. The process is repeated and resultant offspring's inferred phylogenies are compared to determine the rate of recombination that creates a conflicting or supported tree. The program is written in Java and in addition to the simulation has a visualization component to display the pedigrees created.

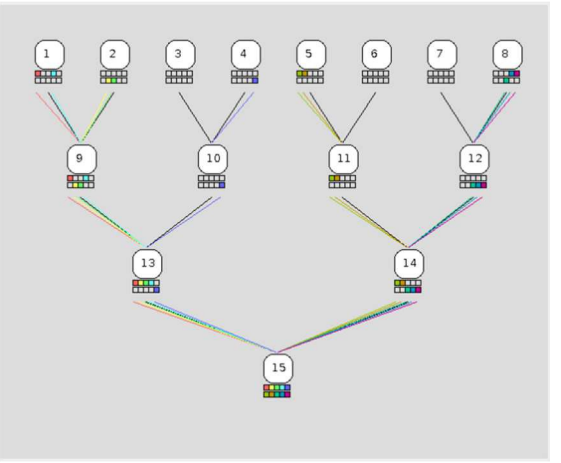

Figure 1: This image is a screen capture of the gui from our recombination software showing the mating of 8 individuals over 3 generations. The colored squares represent a nucleotide sequence of length *n* and the colored lines show from which parent and chromosome the sequence was inherited from. Recombination occurs based on a user specified recombination rate along with the specified distance between each nucleotide sequence.

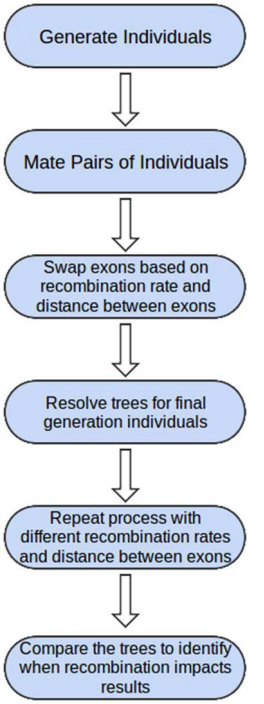

Figure 2: The flowchart here shows the proposed method for determining the effect different recombination rates and distances between exons have on phylogenetic trees. The process depicts simulating individuals, mating them while exchanging alleles through recombination, generating gene trees for the final generation's individuals, and repeating the process. Once this is completed for multiple runs we determine how closely the generated trees support the underlying evolutionary history.

Evan Cresswell
Ph.D. in Computational Science
Advisor: *Gordon Erlebacher*

Astrocyte compartmentalization

Several contemporary studies show that astrocytes, a type of glial cell, are fundamental to several neural functions ranging from metabolic support to higher cognition such as recollection memory. This has resulted in the introduction of astrocytic dynamics into neural modeling. Most cellular function in the astrocyte is triggered by an increase or decrease in calcium concentration within the cytosol. Previous work considered astrocytic dynamics by representing calcium concentration as a point source or a completely spatial model in the cell. We now know, more than ever, that the role of the astrocyte takes many different perspectives. This work, which is inspired by in vivo recordings of astrocytes in the ferret visual cortex, puts forward a novel approach to modeling the different levels of astrocytic calcium activity in the astro-neural system. In the model, we introduce a compartmentalized astrocyte with the purpose of understanding intra-cellular calcium dynamics. Compartmentalizing the astrocyte's

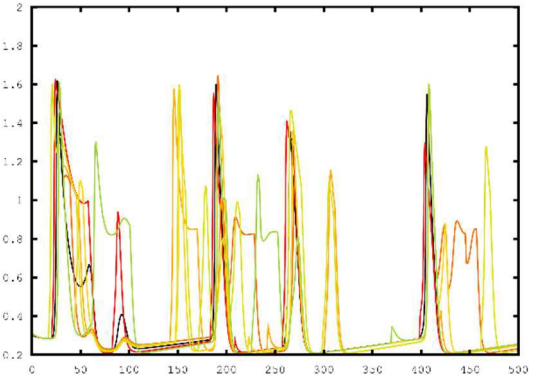

cytosol into the soma and individual branches captures the effect of the local dynamics while still holding on to the analytical power of ODE's. With this model we investigate the interaction between local and global cellular dynamics within the astrocyte in response to neural activity. This allows us to better understand the effect that astrocytes can have on both individual neurons and populations of neighboring neurons.

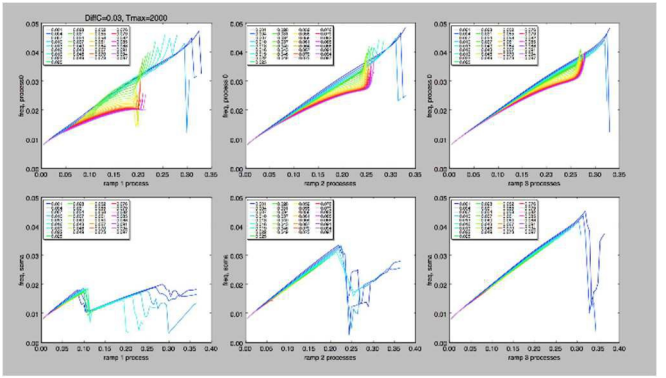

Above: Astrocytic calcium concentration in time

Left: Calcium oscillation analysis

Nathan Crock
Ph.D. in Computational Science
Advisor: *Gordon Erlebacher*

Spatiotemporal patterns of neural activity as the foundation of memory

What are memories? How are they formed and how are they represented in the brain? From classic neuroscience principles, such as neuronal dynamics and synaptic plasticity, complex spatiotemporal patterns of neuronal activity emerge in large networks. It is my contention that these spatiotemporal patterns are the fundamental building blocks of memory. I am interested in understanding the rules and mechanics involved in the formation of these patterns, and exploring how they can interact and combine to form larger, more complex patterns. To the best of my knowledge, there do not yet exist mathematical tools for exploring these phenomena. The activation of a neuron is a nonreversible process and these spatiotemporal patterns only exist while being activated. Therefore any tools capable of shining light on these spatiotemporal patterns will have to address this temporal causality, as well as the combinatorial nature of neural activity. I am developing a set of mathematical and computational tools to explore these questions.

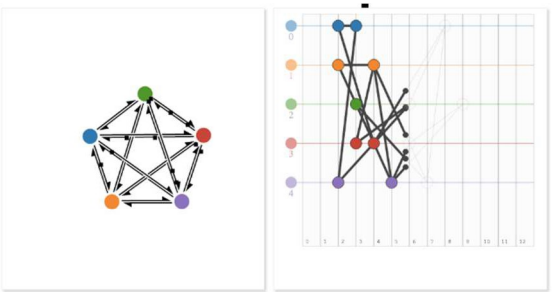

A neural network is represented as a weighted directed graph where each element is a set of times. The times describe how long it takes for a signal from one neuron to reach another. This is the spatial component. The temporal component is introduced using a pseudo time-shift operator. Syntactically, this looks similar to matrix vector multiplication but each element of the matrix and vector is a set. I call this operation the "activation" and it produces another matrix of sets where the elements in a set are the times each signal arrives at that particular neuron. I have also introduced the notion of basis neurons which allow these activities, matrices of sets, to be decomposed into a sum of neuron activations. This mathematical exploration has lead to a succinct recursive expression describing the evolution of activity in a network. The computational implementation of this expression results in an algorithm that is intrinsically adaptive and extremely parallelizable.

$$A_0 = N(t_0)$$
$$A_{n+1} = *(A_n) + N(C(A_n))$$

Figure 1, Left: A screenshot of an interactive visualization of the formation of a spatiotemporal pattern for a particular network.

Figure 2, Above: The equation is a recursive expression which governs the temporal evolution of a network given a particular set of activation times.

Benjamin Crysup
Ph.D. in Computational Science
Advisor: *Sachin Shanbhag*

Uncertainty quantification of dynamical properties in interacting systems

Running molecular dynamics simulations can be expensive. After running one and obtaining a value of interest, there remains the problem of finding the error in the quantity, and it's not immediately obvious how to do this without running multiple simulations. An alternative method for extracting error from one simulation by performing bootstrap sampling on the atom trajectories has been proposed, and previous work has shown that bootstrap sampling works if the atoms in the simulation have independent trajectories.

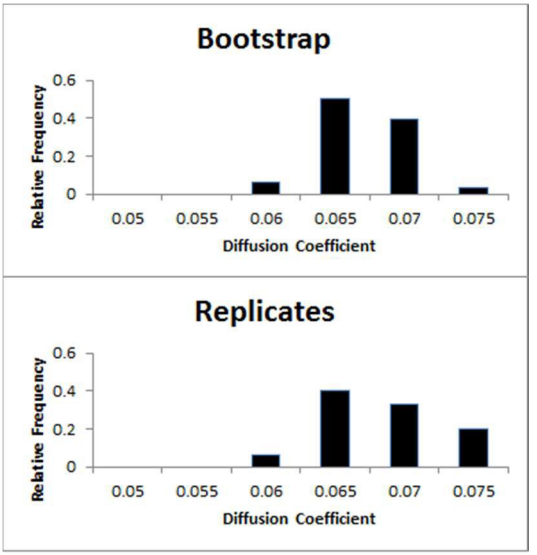

Histograms: Distribution of diffusion coefficients obtained by running replicate simulations compared with taking bootstrap samples from a single simulation.

However, most molecular dynamics simulations have particles that interact, which breaks the assumption of independence made by bootstrapping. In order to test whether bootstrapping is still useful in the absence of independence, a simulation using a common pairwise force (Lennard-Jones) was run at a moderate density, and then the diffusion coefficients of the atoms in the simulation was computed from examining both mean square displacement and velocity autocorrelation, and the error was extracted using bootstrapping. This was compared to the error obtained by running replicates of the simulation. The error was decreased but was still of the same order of magnitude, meaning that, for simulations as expensive as molecular dynamics, bootstrapping still has diagnostic value.

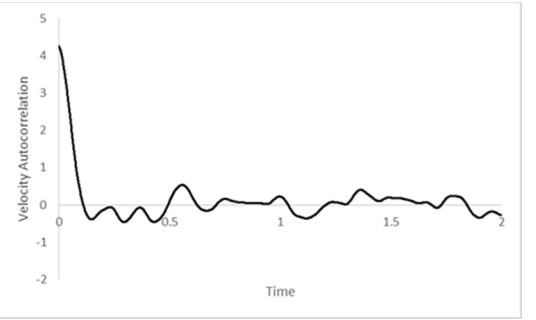

Above: The velocity autocorrelation of a Lennard-Jones simulation.

Anahid Ehtemami
M.S. in Computational Science
Advisor: *Anke Meyer-Baese*

Functional connectivity analysis of resting-state fMRI networks in nicotine dependent patients

Brain imaging studies identified brain networks that play a key role in nicotine dependence-related behavior. Functional connectivity of the brain is dynamic; it changes over time due to different causes such as learning, or quitting a habit. Functional connectivity analysis is useful in discovering and comparing patterns between functional magnetic resonance imaging (fMRI) scans of patients' brains. In the resting state, the patient is asked to remain calm and not do any task to minimize the contribution of external stimuli. The study of resting-state fMRI networks have shown functionally connected brain regions that have a high level of activity during this state. In this project, we are interested in the relationship between these functionally connected brain regions to identify nicotine dependent patients, who underwent a smoking cessation treatment.

Our approach is on the comparison of the set of connections between the fMRI scans before and after treatment. We applied support vector machines, a machine learning technique, to classify patients based on receiving the treatment or the placebo. Using the functional connectivity (CONN) toolbox, we were able to form a correlation matrix based on the functional connectivity between different regions of the brain. The experimental results show that there is inadequate predictive information to classify nicotine dependent patients using the SVM classifier. We propose other classification methods be explored to better classify the nicotine dependent patients.

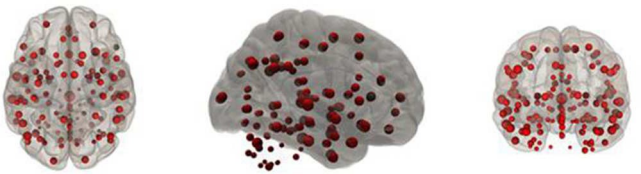

Figure 1. (Left) Dorsal view; (Middle) Medial view; (Right) Posterior view. Shown are the 137 ROIs used to extract the BOLD time series used for the functional connectivity analysis.

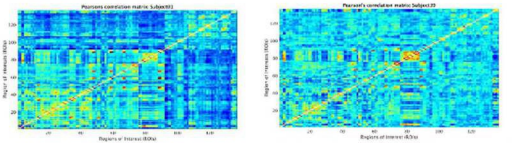

Figure 2. Examples of Pearson's correlation matrix generated for each subject based on each region's BOLD time series correlated with every other region's BOLD time series. The coefficients were z-transformed using Fisher's transform.

Daniel Fenn
Ph.D. in Computational Science
Advisor: *Tomasz Plewa*

Evidence for thermonuclear supernovae from mergers of heavy white dwarfs

This research centers on Type Ia supernovae (SNe Ia), whose origins remain poorly understood. We are exploring the viability of white dwarf binary mergers as progenitor systems for SNe Ia. A close system of two white dwarfs may emit gravitational waves, slowly losing angular momentum and resulting in a gradual inspiral. As the stars approach one another, strong tidal interactions occur, and eventually the less massive star will overflow its Roche lobe. Consequently, its mass will be accreted by the more massive companion.

The infalling accretion stream causes a boundary layer of shocked material to form around the accretor. The shock heating in this region leads to the possibility of thermonuclear fusion conditions. If a sufficient amount of material begins to undergo fusion, a self-sustaining nuclear burning front, or detonation, may propagate through the star. The resulting release of enormous quantities of energy may result in complete disruption of the star as a supernova. Even if boundary layer conditions are not suitable for igniting such a reaction, the possibility still exists for ignition in the accretor's core by way of gravitational compression and heating, resulting from continued accretion.

Figure 1: The early stages of a white dwarf merger.

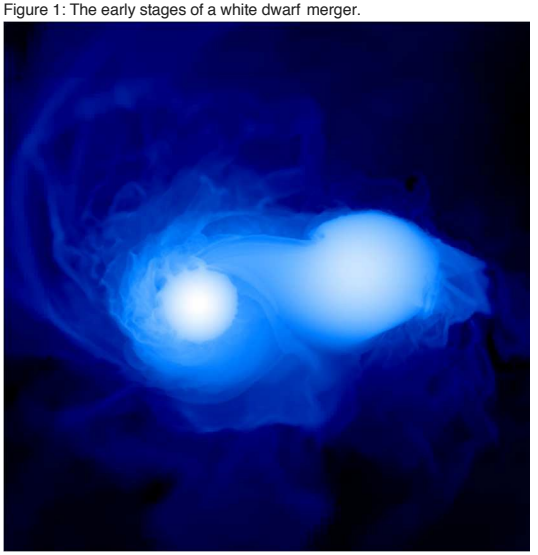

Figure 2: Merger of massive white dwarfs.

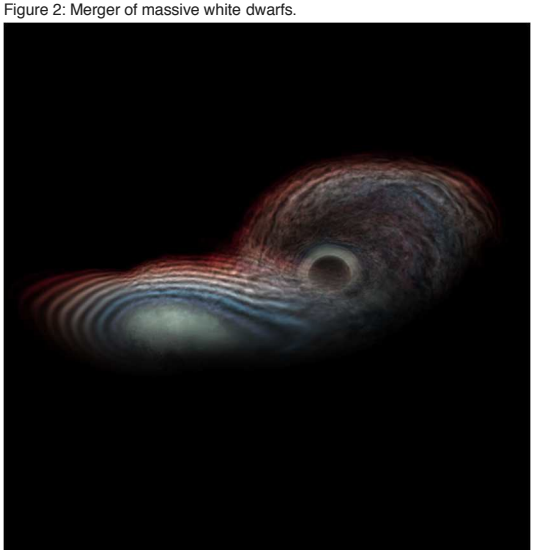

Angtigoni Georgiadou
Ph.D. in Computational Science
Advisor: *Tomasz Plewa*

Evolution and Structure of Massive Stars

The nearby core-collapse supernovea (CCSNe) such as SN 1987A and SN 1993J continue providing valuable constraints on the late evolution of massive stars. Supernova SN 1987A in particular provided quite a few observational 'firsts' such as a detection of neutrinos produced during the core collapse, evidence for asphericity of the explosion and mixing of the ejecta, as well as information about structure of the surrounding interstellar medium. The observations of neutrinos in particular confirmed the core-collapse mechanism of Type II SNe explosions. The aim of this project is to provide information about progenitor stars of selected CCSNe with focus on SN 1987A, SN 1993J, and Cas A. To this end, we will combine stellar evolution models with constrained optimization approach to identify the key model parameters, their most probable values and their observationally constrained ranges. We will consider both a single star and binary star formation channels as certain characteristics of SN 1987A and SN 1993J indicate that they originated from binary systems; rotation was almost certainly a contributing factor in developing jet-like features observed in Cas A. Such optimal progenitor models will then be used as initial conditions for multidimensional computer simulations that will provide input data to the future core-collapse supernova explosion models.

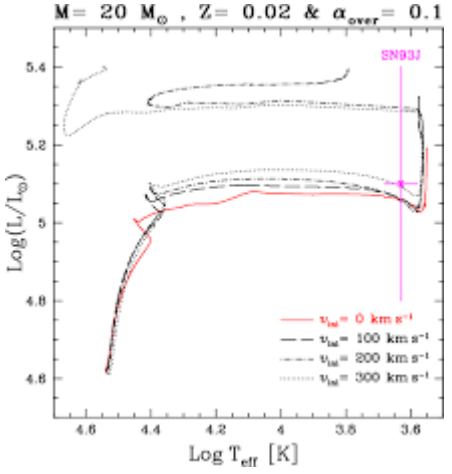

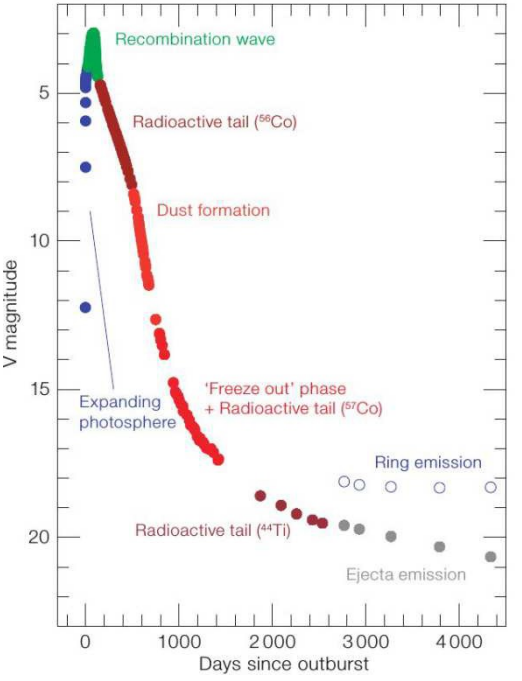

Figure 1, Left: The picture shows the evolutionary track in the HRD for different mass choices for the progenitor star of SN 1987A- Both miss the goal state, denoted by the star symbol.

Figure 2, Above: This graph shows the light curve of the SN 1987A over the first 12 years after explosion.

Brett-Michael Green
Undergraduate in Computational Science
Advisor: *Janet Peterson & Bin Chen*

Simulated Gravitational Microlensing from a Star Field using Raycasting Methods

Light is deflected when propagating in curved spacetimes according to Einstein's general theory of relativity. Multiple images can be formed when a distance source is lensed by a foreground compact object along the line of sight, such as a galaxy or a cluster of galaxies. The gravitational light bending caused by a stellar-mass lens is at the micro-arcsecond level, and is called micro-lensing. A source and compact lens aligned with each other form the Einstein Ring phenomena, where a circular image occurs around the lens with the radius of the Einstein angle. Moving the lens away from the angle from the observer to the source causes the ring image to be distorted into two disconnected elliptic images centered along the axis to the source. If the lens is farther away, or the mass is smaller, the magnification of the image near the source axis becomes stronger, and the image outside the Einstein ring tends to zero as these limits are reached. Multiple lenses having a micro-lensing effect will form a caustic structure, with the lenses heavier and nearer to the source having a greater effect. Using numerical ray-tracing techniques, multiple images in a gravitational micro-lensing system can be found. This provides a method to discover and constrain the physical properties of faint extragalactic objects. We present a proof of concept with a simulation of the gravitational micro-lensing of a background quasar by the random star field in a foreground lens galaxy. The simulation is CPU-expensive, and will be run with parallel computing techniques.

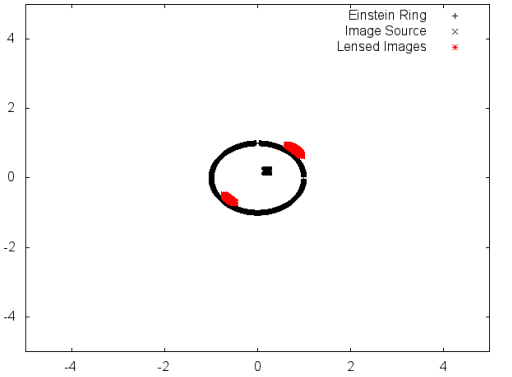

Figure 1: Einstein Ring demonstration, the black ring represents the image if the source and the lens (here centered at 0,0) were aligned. The red shapes are the lensed images, notice that one image is within the Einstein Ring and that the other is not.

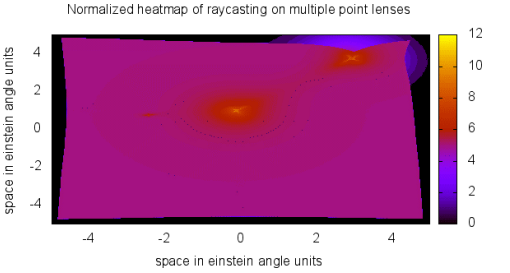

Figure 2: This is a heatmap from the raycasting against three randomized star lenses, it is normalized according to the magnitude, which is logarithmic in scale.

Qingguang Guan
Ph.D. in Computational Science
Advisor: *Max Gunzburger*

Collocation method for one dimensional nonlocal diffusion equations

In this paper, collocation method for solving one dimensional steady state and time dependent nonlocal diffusion equations is analyzed. The difficulty of applying collocation method to nonlocal diffusion equations comes from the singularity of the kernel. If s < ½ it is weakly singular integral, however, if s>½ the integral is not integrable in Riemann sense, so the Hadamard finite part integral is introduced to overcome this difficulty. But new things bring new troubles. For analysis and performance, a "balance" term is added to discretize the nonlocal operator. Numerical results support the theorems.

Example 1.
Let $u(x) = x^2(1-x^2)$, then

$$-\mathcal{L}_\delta u = \frac{2-2s}{\delta^{2-2s}} \int_{x-\delta}^{x+\delta} \frac{u(x)-u(y)}{|x-y|^{1+2s}}\, dy = (12x^2-2) + \frac{2s-2}{s-2}\delta^2$$

Table 1: Numerical results ($\delta = 0.1, s = 0.4$)

n	$\|e\|_\infty$	ratio	$e_{truncation}$	ratio	$\|\mathcal{A}\|_\infty$
7	2.135781e-01		2.468391e+00		3.169786e-01
15	1.863756e-01	0.197	1.287209e+00	0.939	6.143939e-01
31	1.428161e-01	0.384	6.106285e-01	1.076	1.060865e+00
63	9.306979e-02	0.618	2.775233e-01	1.138	1.566544e+00
127	5.189687e-02	0.843	1.234706e-01	1.168	1.986530e+00
255	2.581967e-02	1.007	5.438204e-02	1.183	2.255554e+00
511	1.201548e-02	1.104	2.391942e-02	1.185	2.401109e+00
1023	5.400836e-03	1.154	1.048225e-02	1.190	2.473039e+00
2047	2.386882e-03	1.178	4.584957e-03	1.193	2.507105e+00
4095	1.046428e-03	1.190	2.002777e-03	1.195	2.522957e+00

Table 2: Numerical results ($\delta = 0.1, s = 0.6$)

n	$\|e\|_\infty$	ratio	$e_{truncation}$	ratio	$\|\mathcal{A}^{-1}\|_\infty$
7	1.362766e+00		1.737165e+00		2.891150e+00
15	5.026394e-01	1.439	1.142448e+00	0.605	1.914829e+00
31	1.533591e-01	1.713	6.988938e-01	0.709	1.043245e+00
63	6.948869e-02	1.142	4.131606e-01	0.758	8.370253e-01
127	3.560824e-02	0.965	2.406352e-01	0.780	7.528877e-01
255	1.925267e-02	0.887	1.391594e-01	0.790	7.115317e-01
511	1.069229e-02	0.848	8.019510e-02	0.795	6.894626e-01
1023	6.025212e-03	0.827	4.613623e-02	0.798	6.772092e-01
2047	3.423004e-03	0.816	2.651998e-02	0.799	6.702679e-01
4095	1.953681e-03	0.809	1.523790e-02	0.799	6.662955e-01

Ryan Learn
Ph.D. in Computational Science
Advisor: *Tomasz Plewa*

Numerical Simulations of Transport Processes in Plasma Instabilities

In the study of complex fluid flows in any context, understanding and accurate modeling of turbulent behavior of such flows is of crucial importance. The effects of shear, buoyancy, and impulsive acceleration can be qualitatively discussed using the results of perturbation analysis in the initial linear phase of evolution, but soon the evolution of such systems is dominated by nonlinear effects and turbulent mixing. This highly perturbed, turbulent flow requires direct numerical simulation for accurate modeling of systems of astrophysical importance, such as accreting neutron stars and white dwarfs, as well as the massive explosions of Type Ia and II supernovae.

Our work is focused on the implementation of numerical models for various physical processes that effect the evolution and growth of shear and buoyancy driven instabilities. We validate these models through comparison with instability growth rate predicted by perturbation theory during the linear phase of instability growth. Once validated, these numerical models will be used to study the nonlinear evolution of such instabilities in various regimes, allowing us to quantify the role these instabilities play in the dynamics of astrophysical processes. Such numerical studies will also make strides toward the development of various sub-grid and parameterized models for instabilities, allowing for accurate modeling of mixing due to such instabilities that may otherwise be unresolvable on even the fastest of current generation computing hardware.

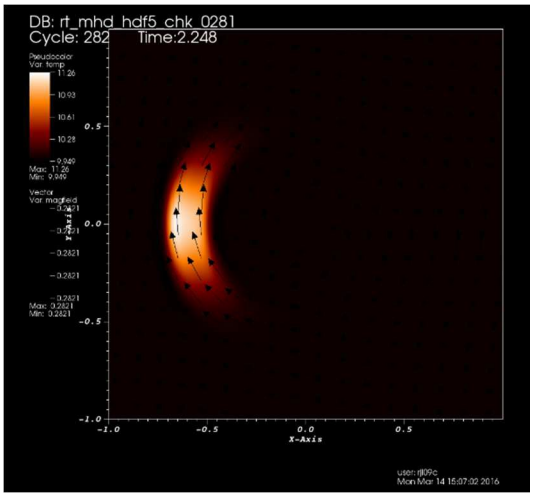

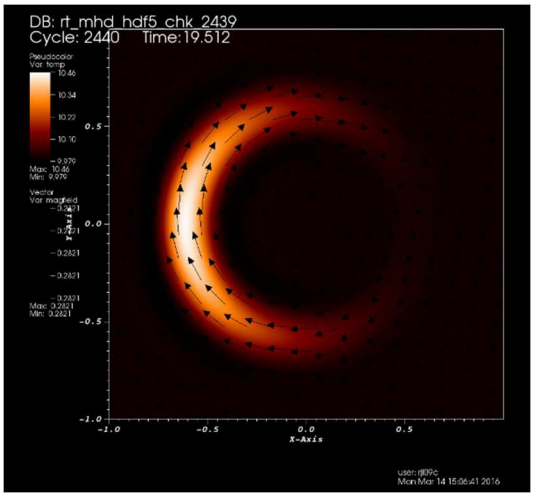

Images: Evolution of temperature profile in uniform plasma in the presence of anisotropic thermal conductivity due to the presence of a cyclically oriented magnetic field.

Isaac Lyngaas
Ph.D. in Computational Science
Advisor: *Janet Peterson*

Using Radial Basis Functions to Solve a Nonlocal Model for Anomalous Diffusion

Nonlocal diffusion models differ from traditional models by replacing the spatial derivatives in the PDE model with an appropriate integral. In many applications (e.g., biological systems, flow through porous media) the observed rate of diffusion is not accurately modeled by the standard diffusion differential operator but rather exhibits so called anomalous diffusion. This diffusion can be represented in a standard PDE model by using a fraction Laplacian. However, in the nonlocal approach the integral only needs to be slightly modified so the solution method is virtually the same for standard or anomalous diffusion. Solving anomalous diffusion problems is a very active research area and using a nonlocal model is a very promising approach.

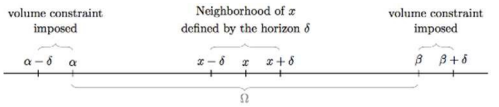

Figure 2: Domain defined for a one-dimensional nonlocal problem.

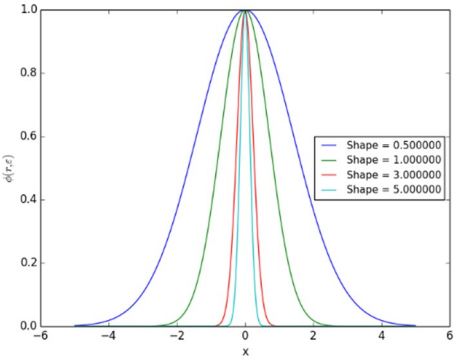

Figure 1: Gaussian RBF as the shape parameter varies.

In this work we propose using radial basis functions (RBFs) to derive a quadrature rule for approximating the integral appearing in the nonlocal model. RBFs are well known for their ability to interpolate scattered data and their desirable convergence rates. We demonstrate how approximations to the nonlocal integral are obtained using RBFs. Numerical results in one spatial dimension are given and compared with those obtained by using a standard finite element approximation to the nonlocal model.

Alisha Rossi Mechtley
Ph.D. in Computational Science
Advisor: *Alan Lemmon*

Automated Workflow for Mitochondrial DNA Extraction and Analysis from High Throughput Sequencing Data

Next-generation sequencing data are rich in information and contain many off-target sequences (reads), including mitochondrial reads, that are often ignored but which may be biologically relevant. Mitochondrial DNA (mtDNA) is now providing new perspectives on the tree of life and the etiology of the common complex diseases. The mtDNA codes for important bioenergetic genes has a very high mutation rate, and can be present in thousands of copies per cell. My research utilizes current de-novo and referenced based methods of mitochondrial genome extraction from high throughput sequencing data. I implement a workflow to map reads gathered using anchored phylogenetics from a popular next generation platform (Illumina) to taxonomically related species genes in a relational database in order to extract the mitochondrial genes.

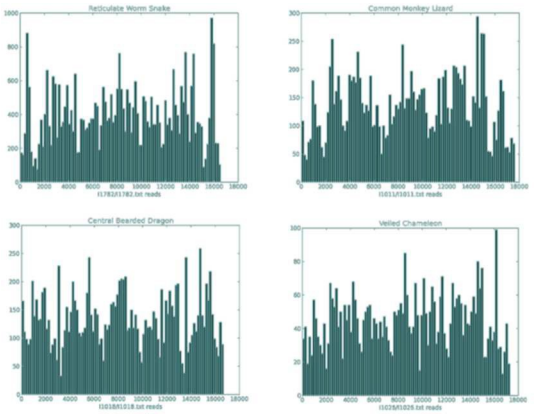

Figure !: The number of mitochondrial reads versus the mapped location (in base pairs) for four vertebrates in anchored phylogenomic studies.

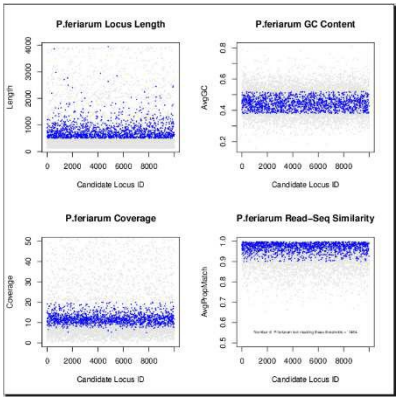

Figure 2, Above: Various criteria for selecting anonymous loci for use as genetic markers in probe kits. Loci are individually judged by length, GC content, sequence coverage, and read-seq similarity. Acceptable loci (blue) must be within a certain threshold specific to the given criteria.

Marcelina Nagales
Undergraduate in Computational Science
Advisor: *Dennis Slice*

Typology Variability in Southeastern American Projectile Points

This study uses projectile point/knives (PPK's) of different typologies to construct a database of virtual projectile points, manual measurements, and other details concerning the point to help classify unknown points with similar features. This database will be the first of its kind to feature complete 3D scans of PPK's for users to manipulate. A database with 3D scans of projectile points has a global significance as it gives broad access to virtual renderings where users can make virtual measurements and interact with the projectile points. Current databases of similar types feature much broader classifications and use 2D images as representations. This study used Flex Scan 3D scanning software and a rotary table to scan the artifacts held at the Florida Bureau of Archaeological Research. All of the PPK's were found and are associated with the Southeastern United States. Several scans were taken of each projectile point from different angles to ensure the entire surface was scanned accurately. Additionally the scans were combined and finalized in a readable format. A unique system was devised for manually measuring PPK's of different typologies (both Clovis and stemmed) and each point was measured accordingly using similar landmarks. These landmarks will be used in a future study of changing morphology among Southeastern PPK typology. Previous studies have used the Flexscan 3D scanning software to aid in archaeological preservation, while others have used the same scanning software to scan macerated bones to recreate animal skeletal structures.

Figure 1: A Citrus type projectile point/knife with a scale.

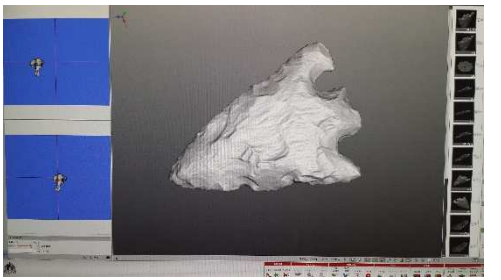
Figure 2: The same Citrus type projectile point/knife on the Flexscan 3D software.

Ben Pomidor
Ph.D. in Computational Science
Advisor: *Dennis Slice*

Automated Classification of Cranial Shape from Fragmentary Remains

Certain biological markers, such as intentional modification to the crania and dentition, have the unique potential to provide information about ethnicity, kinship, and social identity. Cranial modification in particular offers a rare glimpse into intra- and inter-population dynamics because of its physical and permanent impartment of identity on the skeleton during childhood. However, data collection of culturally modified crania in pre-Columbian populations is commonly limited by poor preservation, inhibiting visual assessment of cranial shape. Cranial shape determination of fragmentary remains can increase sampled individuals and thus enhance analyses of mortuary datasets.

In this project, an automated method of computational shape analysis was developed and applied to surface scans of cranial fragments (n=17) from the Mississippian Period cemetery of Bull Creek (9ME1) —a population that exhibits fronto-parieto-occipital flattening of the crania as well as individuals with unmodified crania. The method uses a novel surface-clipping algorithm to extract a roughly homologous pseudo-fragment from the surface scan of a visually identified complete skull.

In the second half of the method, the shape difference values are used to determine the presence/absence of modification for each fragment. A data set made up of six of the cranial bones of each prototype skull, combined with eight previously identified fragments, was used for training and validation. Better evaluation of such remains facilitates the bioarchaeological exploration of cultural identity.

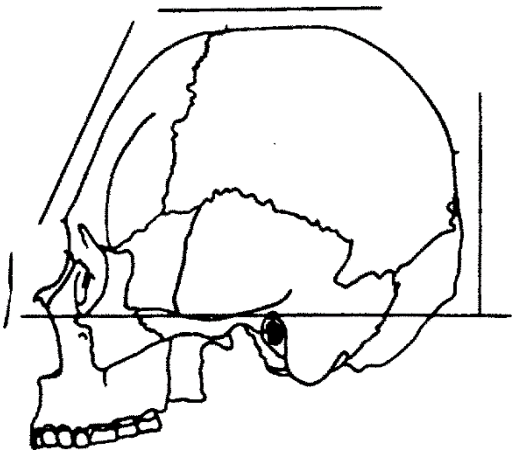

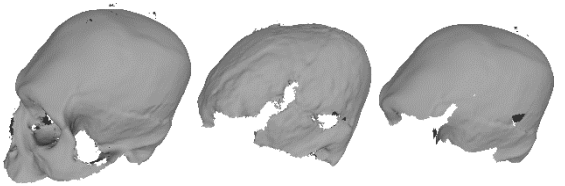

Figure 1, Left: Surface scan of prototype modified skull (left), fragment used for clipping (center), and resulting pseudo-fragment of modified skull (right).

Figure 2: Above: Fronto-parieto-occipital modification. Image from Neumann 1942.

Michael Schneier
Ph.D. in Computational Science
Advisor: *Max Gunzburger*

An Ensemble-Proper Orthogonal Decomposition Method for the Nonstationary Navier-Stokes Equations

The definition of partial differential equation (PDE) models usually involves a set of parameters whose values may vary over a wide range. The solution of even a single set of parameter values may be quite expensive. In many cases, e.g., optimization, control, uncertainty quantification, and other settings, solutions are needed for many different sets of parameter values. We consider the case of the time- dependent Navier-Stokes equations for which a recently developed ensemble-based method allows for the efficient determination of the multiple solutions corresponding to many parameter sets. The method uses the average of the multiple solutions at any time step to define a linear set of equations that determines the solutions at the next time step. To significantly further reduce the costs of determining multiple solutions of the Navier-Stokes equations, we incorporate a proper orthogonal decomposition (POD) reduced-order model into the ensemble-based method. The stability and convergence results previously proven for the ensemble-based method are extended to the ensemble-POD approach. Numerical experiments are provided that illustrate the accuracy and efficiency of computations determined using the new approach.

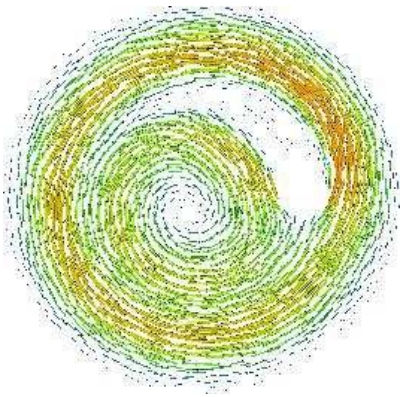

Figure 1: The velocity field of our ensemble – POD model

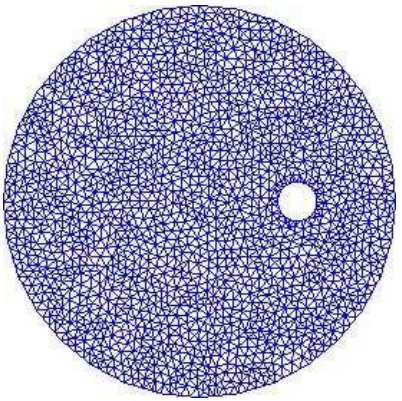

Figure 2: 16000 degrees of freedom mesh which we use in the calculations of the ensemble POD algorithm.

Maliheh Shaban-Tameh
Ph.D. in Computational Science
Advisor: *Chen Huang*

Investigation of Surface Catalysis with the Density Functional Embedding Theory

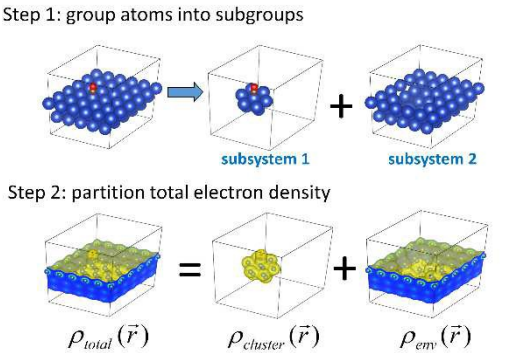

We focus on two important surface catalytic processes: the methanol synthesis from the syngas ($CO/CO_2/H_2$) on copper and the Fischer-Tropsch process from the syngas on iron. We investigate these two industrially important processes using the density functional embedding theory (DFET). DFET is a multi-scale method for obtaining accurate reaction energies of surface catalysis. DFET has been successfully employed to many challenging surface problems, such as explaining the adsorption of carbon monoxide on copper surface, resolving the controversial mechanism of the aluminum oxidation, and shedding light on the plasmon-assisted hydrogen dissociation on gold nanoparticles. The basic idea of DFET is that we partition a system's electron density into subsystem densities. After the partitioning, the region of interest (ROI) is defined and is solved by a high-level method, with the environment replaced by a local embedding potential. In this work, we generalize DFET to spin-polarized materials to study the Fischer-Tropsch process in which the catalyst is iron. The key quantity in DFET is the embedding potential that represents the interaction between the ROI and its environment. We develop a robust embedding potential solver for calculating the embedding potential. High-quality embedding potentials are obtained. The efficient embedding potential solver developed in this work can let us study the outer layer of a catalyst with high-level theories by replacing the subsurface with a first-principle, spin-polarized embedding potential, which substantially reduces the computational cost. In this work, we employ high-level Kohn-Sham (KS) DFT calculations employing the exact-exchange and the correlation based on the random phase approximation (RPA) to construct the accurate reaction energies of the methanol synthesis over copper and the Fischer-Tropsch process over iron. It is known that the EXX+RPA has a good accuracy in calculating the adsorption energies of molecules on transition metals, however the scaling of its computational cost is poor. By employing embedded EXX+RPA calculations, we can gain insight into the heterogeneous catalysis with a modest computational cost.

Bottom Left The methanol synthesis involves several major chemical reactions: the CO hydrogenation, the CO2 hydrogenation, the water-gas shift reaction (WGSR), and the reverse water-gas shift reaction (RWGSR). In addition, the CO and CO2 hydrogenation can occur at the interface between Cu and ZnO, and/or occurs on the metallic copper. Which one is the dominating pathway, the CO hydrogenation or the CO2 hydrogenation, is still under debate.

Top Right: The two-step partitioning in the density-functional embedding theory.

Danial Smith
Ph.D. in Computational Science
Advisor: *Gordon Erlebacher*

Player Modeling and Procedural Content Generation

Education fails if students remain passive. Educational games teach because they activate students. In an ideal case, each student would be best served by a game specifically adjusted to that student's background and learning speed. Games tailor-made for each individual would be costly to create by hand. Adaptive procedural methods allow for that to become a reality. Using procedural content generation methods, logging of player actions, and Bayesian analysis of these actions two adaptive games are being created to focus on the player's perceived interests or to increase their skill in some subject. The first, Preempting Path, is a series of procedurally generated mazes created. The player is judged on time to completion and percentage explored. After completion of a maze, the next will be slightly more difficult for that person's play style. The second, e-Rebuild, focuses on assisting children around age 12 with mathematical concepts such as ratio/proportion and geometry. The difficulty of each level will be based on the player's mastery of the competency being assessed. This game uses remote analysis of the players actions, and as a result the game adapts less often. While still in its infancy, the game is regularly tested by a class of seventh graders at Florida State University Schools. Results are limited from this testing, but it is clear the students have no objection to playing games during class time.

Figure 1: The start screen for the game e-Rebuild.
.

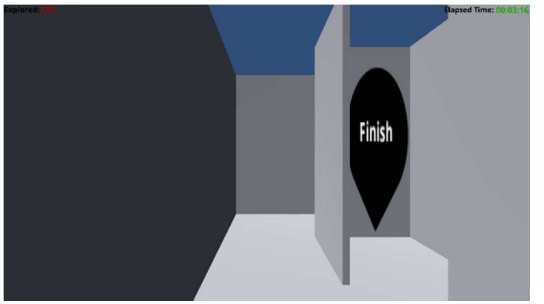

Figure 2: End screenshot of one of the procedurally generated levels.

Kenneth C. Sockwell

M.S. in Computational Science

Advisors: *Janet Peterson & Max Gunzburger*

Passing Resistance Free Transport Currents Through Two Band-Superconductors

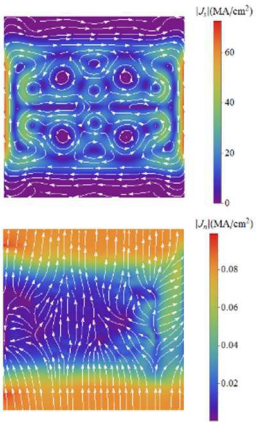

Developing simulations of vortex pinning in superconductors is crucial in designing efficient superconducting technology and material characterization of superconductors. One promising application of superconductors is transporting an electrical current with no electrical resistance. Unfortunately the amount of resistance free current is limited by the movement of magnetic flux tubes, or vortices, that are induced from the magnetic field associated with the electrical current. The vortices are comprised of magnetic flux that penetrates the sample in thin, long tubes. When magnetic flux passes an electrical current, the vortices interact with it, creating electrical resistance; this destroys the integrity of the superconductor. This catastrophic interaction can be prevented by immobilizing the vortices through a process know as vortex pinning. Experimentally this is done by introducing impurities into the superconducting sample. In simulations, this is captured by using different material parameters in the geometry where the different metals are located. In this work simulation results are shown that model the passing of a resistance free current through a two-band superconductor with impurities in the sample. The simulation uses the Two-Band Ginzburg Landau model to describe vortex dynamics in the superconductor as well as the

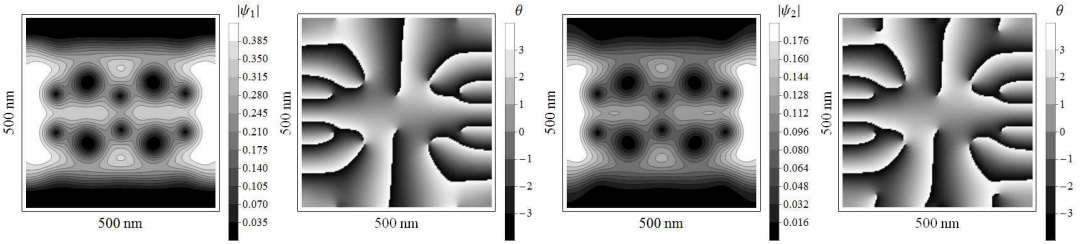

vortices' interaction with the impurities and normal inclusions. When an electrical current is passed through the sample, the simulation can provide the resistance free and resistive components of the current. The effectiveness of the vortex pinning impurities can then be evaluated by finding the increase in resistance free current in sample when compared to pure samples.

Figure 1, Top Right: The resistance free component of the electrical current (top) and the resistive component of the electrical current (bottom). The resistive component is very high in the normal metal bands but drops significantly in the superconducting sample due to vortex pinning in the superconductor. The current is passed as resistance free current throughout the superconducting sample. However most of the resistance free current is induced from the magnetic field and is not transported through the samples, but circles inside of it.

Figure 2, Above: Contours of the order parameter, psi, and their complex phase, theta, of the first superconducting band (left two) and the second superconducting band (right two) in Magnesium Diboride, while an electrical current is applied to the sample in the upward direction. Normal metal bands are placed at the top and bottom of the sample to introduce and remove transport currents. There are four impurity metal inclusions (large black circles), which server as vortex pinning sites, as well as several vortices (small black circles).

James Soda
Ph.D. in Computational Science
Advisor: *Dennis Slice*

An Implementation of Newton-Raphson Optimization to provide Maximum Likelihood Estimates of Vector Autoregressive-moving Average Models in an R environment

Vector autoregressive-moving average (VARMA) models are one of the most common families of models in multivariate time series analysis. Unfortunately, there are only a few programs and routines available to estimate VARMA models, and even these options have some undesirable features. Many available options will only provide estimates in standard format, which allows the same time series to map to multiple, observationally equivalent models. As such, two sections of the same stochastic process could map to two seemingly disparate models, creating the illusion of separate processes. Another undesirable feature is an inability to arrive at estimates for certain time series. One challenge to arriving at estimates arises because there is a limited region in which the model fits an assumption of VARMA models called invertibility. If an iterative method proposes a non-invertible model, the routine may crash as the values that are needed to generate the next iteration become unreasonably large. As such, a maximum likelihood routine is more likely to obtain an estimate if there is a subroutine to assess the invertibility of a proposed model and to reject the model if it is inappropriate. Unfortunately, such a subroutine would need to estimate the roots of a matrix polynomial's determinant, which is a challenge in and of itself. Here we discuss a routine for the R environment that uses a Newton-Raphson algorithm to maximize the conditional likelihood of certain VARMA models. Based on the suggestions in Reinsel (1994), we adjust the Newton-Raphson algorithm to estimate models in reverse canonical echelon form, thus guaranteeing uniqueness of the model. Further, we convert the root finding problem needed to assess invertibility into an eigenproblem. Then, we demonstrate this routine is able to arrive at feasible models for simulated time series whose true model structure is known via likelihood ratio tests and compare its performance to existing options. Finally, we discuss the limitations of this implementation and what future features will be added.

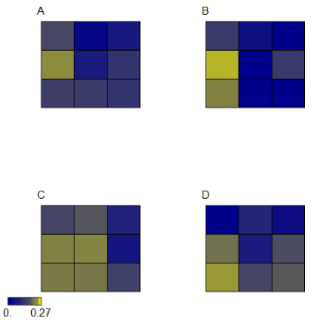

Figure 1. Heat maps indicating the absolute differences between the true model and our routine's estimate for the model.

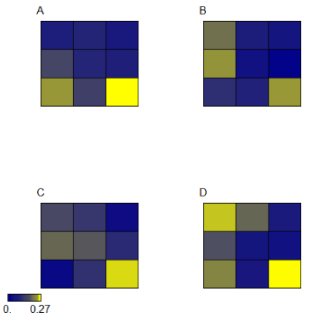

Figure 2. Heat maps indicating the absolute differences between the true model and an estimated model from Tsay (2015)'s VARMA routine

Stephen Townsend
M.S. in Computational Science
Advisor: *Dennis Slice*

Geographic Variations in Animal Vocalizations Using a new Method in Spatial Analysis

Animal vocalization is a major area of research in modern ecology. Vocalizations play many important roles in the lives of the animals that inhabit our planet, from warning of danger to finding a mate. There exist patterns of spatial variation in these

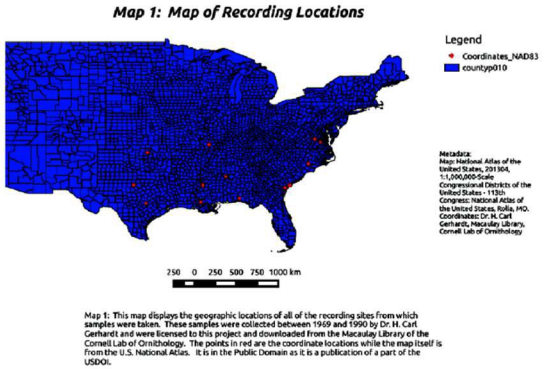

vocalizations which have been very well documented time and time again. In some cases, the differences are so pronounced that they may play a role in reproductive isolation and speciation. Here, we present a new quantitative method for analyzing geographic trends in animal vocalization using frog calls as a model organism to demonstrate the utility of our method. Our method does not rely upon the use of spectrograms, instead it focuses on the shape of the waveform itself as a basis for analysis. To validate our method, a sample of 187 mating calls of the Cope's Gray Treefrog (Hyla chrysoscelis) were downloaded from the Macaulay Library. These calls were then filtered and aligned to ensure shape was the only variable. These aligned and filtered calls were analyzed with dimension reduction and regression methods to determine spatial variation. Using this data, we show that our method is a reliable, novel approach to geospatial bioacoustic analysis.

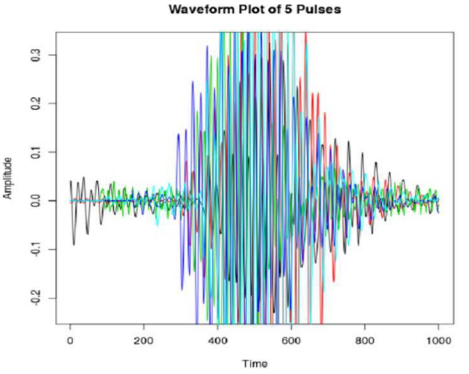

Figure 2: This figure shows a sample of 5 pulses extracted from the frog calls.

David Witman
Ph.D. in Computational Science
Advisor: *Janet Peterson & Max Gunzburger*

Reduced Order Modeling for a Nonlocal Approach to Anomalous Diffusion Problems

With the recent advances in using nonlocal approaches to approximate traditional partial differential equations (PDEs), a number of new research avenues have been opened that warrant further study. One such path that has yet to be explored is using reduced order techniques to solve nonlocal problems. Due to the interactions between the discretized nodes or particles inherent to a nonlocal model, the system sparsity is often significantly less than its PDE counterpart. Coupling a reduced order modeling (ROM) approach to a nonlocal problem would ideally reduce the computational cost without sacrificing accuracy. This would allow for the use of a nonlocal approach in large parameter studies or uncertainty quantification. Additionally, because nonlocal problems inherently have no spatial derivatives, solutions with jump discontinuities are permitted. This work seeks to apply reduced order nonlocal concepts to a variety of problem situations including anomalous diffusion, advection, the advection-diffusion equation and solutions with spatial discontinuities. The goal is to show that one can use an accurate reduced order approximation to formulate a solution at a fraction of the cost of traditional techniques.

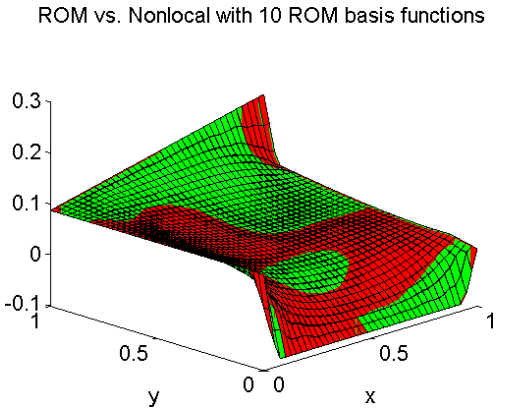

Figure 1: 2D ROM (green) and finite element nonlocal (red) solutions at a defined parameter set.

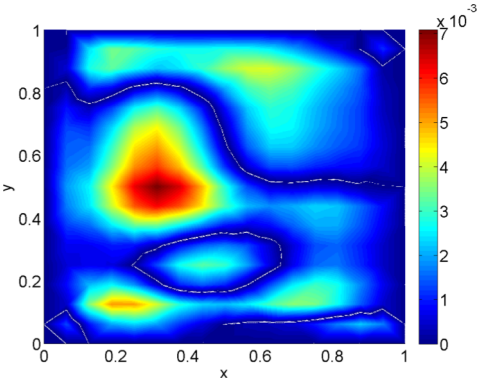

Figure 2: The corresponding point-wise error associated between the reduced order and finite element solutions

Wenju Zhao
Ph.D. in Computational Science
Advisor: *Max Gunzburger*

Stochastic Navier Stokes equation and higher precision simulation of bi-harmonic

This poster includes two parts. In the first part, we provide a regularized method for stochastic Navier-Stokes equations with additive noise. The trace of the noise can be finite or infinite with appropriate regular parameters. The stability and convergence of the path-wise modified Navier-Stokes equations has been proved. The numerical examples are provided to illustrate our schemes. The comparison of non-regularized and regularized noises to the Navier-Stokes systems is presented.

In the second part, we provide high precision computational methods for the bi-harmonic equation. We will use some tables to explain the higher convergence rate. A high oscillating function is simulated; the numerical solution and the exact solution are represented graphically below.

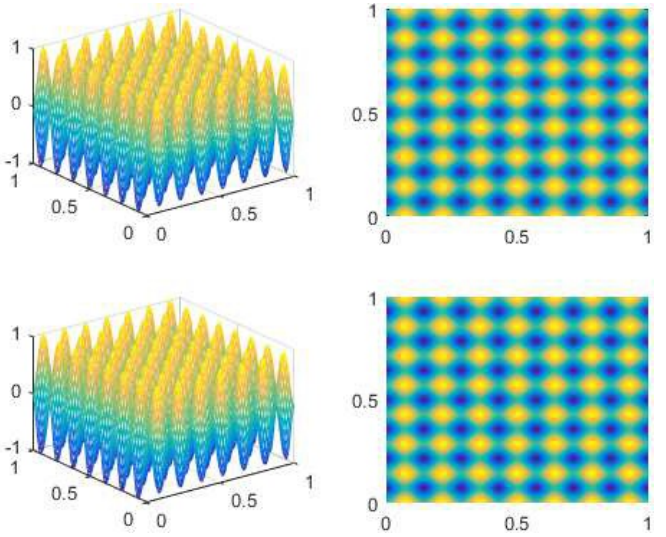

Figures: The first row presents the numerical solution, and the second row represents the exact solution.